

COMPARISON OF KINEMATIC AND THORACIC RESPONSE OF THE 5TH PERCENTILE HYBRID III IN 40, 48 AND 56 KM/H RIGID BARRIER TESTS

Suzanne Tylko
Dominique Charlebois
Transport Canada
Canada
Alain Bussières
PMG Technologies
Canada

Paper Number 07-0506

ABSTRACT

Full-scale crash tests were conducted to investigate the correlation between the 5th percentile Hybrid III dummy kinematics and chest response at three test speeds. A total of 20 comparative full frontal rigid barrier tests were conducted at 40, 48 and 56 km/h with the dummies placed in the front and rear outboard seating positions.

As test speed increases to 56 km/h, the forward excursion and rotation of the thorax increases significantly. This rotation combined with chest jacket distortions inhibits the accurate measurement of chest deflection. The influence of the seat characteristics and belt geometry at peak load are explored.

A new multi-point sensing device, known as the RibEye is introduced in full-scale rigid barrier tests to evaluate the role of multi-point sensing in enhancing the accuracy of chest deflection measurements. This new instrumentation may significantly reduce the sensitivity to belt placement associated with traditional single point measurements.

An impulse calculation method to evaluate the load management capability of restraint systems is proposed.

INTRODUCTION

In 2001 the Government of Canada published in the Canada Gazette, a Notice of Intent to change the Canadian Motor Vehicle Safety Standard for frontal protection (CMVSS 208). The department strives to harmonize motor vehicle safety standards with the U.S., except in cases where harmonization would lead to the relaxation of an existing safety requirement.

The CMVSS 208 currently requires that the peak chest deflections for the Hybrid III 50th male remain below 50 mm for frontal rigid barrier tests conducted

at up to 48 km/h. Complete harmonization with the U.S. FMVSS 208 would mean increasing the allowable chest deflection limit to 63 mm for the male and adopting a limit of 52 mm for the 5th percentile female. Raising the limit for chest deflection to levels that are beyond the magnitudes measured in vehicles would negate the benefit of including chest deflection as an injury criterion. A lower limit scaled to the 50th male is needed for the 5th percentile female.

Transport Canada has been engaged in the conduct of research to investigate the characteristics of the chest under belt and or combined belt and airbag loading conditions to identify the factors affecting chest response in the 5th percentile ATD. A study on the effects of breast anthropometry on chest response was reported in Stapp 2006 (Tylko, S. et al). During the course of this investigation it became evident that chest deflection did not increase linearly between 40 and 56 km/h FFRB tests. The dummy behaved differently at higher test speeds.

As the test speed is increased the extent of forward excursion and rotation about the torso belt is amplified and torsion of the jacket with respect to the rib cage becomes more noticeable. Observation of the high-speed video indicated that the dummies rotated outboard as they approached the limit of forward excursion thus redirecting the load away from the single point measurement sensor in the sternum.

A new multi-point sensing system was added to the instrumentation of the dummy to assist in the characterization of load application. The paper presents the preliminary multi-point measurements and the results of an alternative approach used to investigate the kinematics of the dummy and the influence that this may have on chest response.

METHODOLOGY

Crash Tests

Frontal rigid barrier tests were carried out at 40, 48 and 56 km/h with model year 2006 - 2007 vehicles. The Hybrid III 5th percentile female anthropometric test device (ATD) manufactured by Denton ATD and FTSS were seated in the front and rear outboard seating positions. Test set-up, vehicle preparation, and dummy positioning for the front seat were done in accordance with the respective sections of the FMVSS 208 requirements for the full frontal rigid-barrier tests (FFRB).

The rear doors were removed to provide optimized camera views of the dummy kinematics. Video cameras were attached to the vehicle as shown in Figure 1. Pre and post-test dimensions were obtained to monitor for B-pillar displacement during the test should it occur.

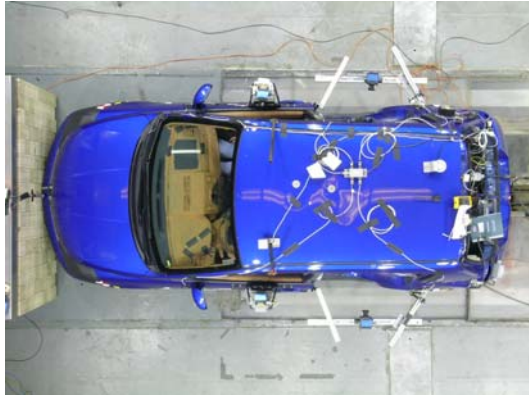


Figure 1: Plan view of camera locations.

Instrumentation and Video Imaging

Data were recorded at 10kHz and filtering was performed in accordance with SAE J211. High-speed videos at 1000 frames/second were obtained and included lateral views of the front seat occupants; lateral and a frontal view of the rear seat occupants. Overhead camera views of the occupants were obtained for one vehicle with a retractable roof (convertible).

The baseline instrumentation in the dummies included a tri-axial accelerometer at the head CG, a 6-axis load cell at the upper and lower neck and lumbar spine; a 3-axis clavicle load cell; tri-axial accelerometers at the upper, mid and lower spine and pelvis; accelerometers at the top mid and lower sternum; and single axis load cells in the femurs. The chest potentiometer was supplemented with either the THUMPER kit consisting of four IR-TRACCs (InfraRed – Telescoping Rod for Assessment of Chest Compression) or the RibEye for multi-point sensing.

RibEye

The RibEye is an electro-optical system developed by Boxboro Systems and Denton ATD for the measurement of rib deflections. The first production version was developed for Transport Canada for use in the 5th Female Hybrid III ATD. The RibEye measures the X and Y locations of 12 points on the ribcage using optical triangulation at a sampling rate of 10 kHz. Light emitting diodes (LEDs) can be attached to the ribs anywhere within the measurement range, offering much greater measurement flexibility than the traditional fixed sensors. Two light angle detectors are mounted on the sides of the spine box while the RibEye controller, is mounted in the spine box. The RibEye controller auto adjusts the brightness of each LED to enhance accuracy. After the angle data is acquired, the controller calculates the X and Y position of each LED by triangulation and reports the data in millimeters with an accuracy of 1 mm.

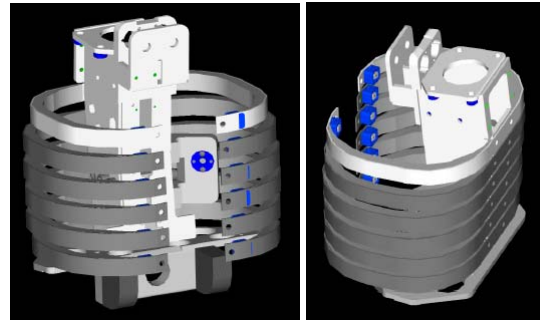


Figure 2: RibEye sensor & light detector location.

RESULTS

RibEye Chest Deflection

Tests were conducted with the RibEye installed in a Denton 5th percentile Hybrid III ATD. The 12 sensors were located on each rib at approximately 60 mm from the centerline of the sternum. By comparison, the four IR-TRACCs are attached at approximately 30 mm from the centerline of the sternum. As shown in Table 1, the majority of the tests were conducted in the rear seat to investigate the RibEye response in belt only loading conditions. Two driver tests were also conducted to evaluate the RibEye performance in combined belt and airbag loading conditions and compare this to the pure belt loading responses.

Table 1: Tests conducted with the RibEye

| FFRB Test Speed | | | |
|-----------------|---------|---------|---------|
| Position | 40 km/h | 48 km/h | 56 km/h |
| 11 | | 1 | |
| 13 | | 1 | |
| 14 | 1 | 1 | |
| 16 | 2 | 1 | 4 |

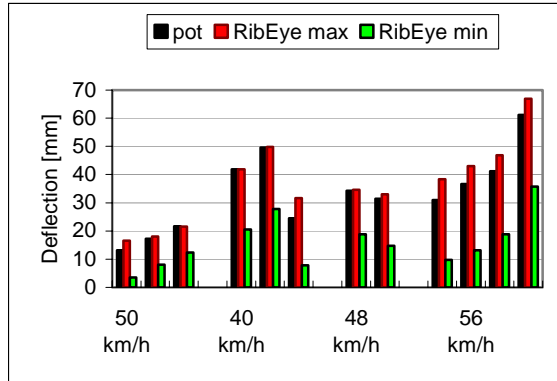


Figure 3: Comparison of peak chest deflection measured at potentiometer to peak RibEye measurement for rear seat, belt only.

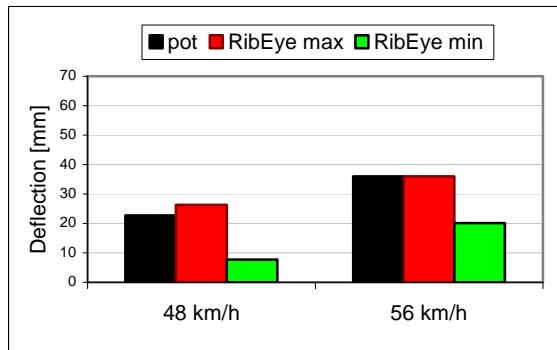


Figure 4: Comparison of peak chest deflection measured at potentiometer to peak RibEye measurements for a driver at 48 and a driver at 56 km/h with belt & airbag.

As can be seen in Figure 3 the discrepancy between the deflection measurement of the potentiometer and the RibEye measurement of the individual ribs increases as test severity is increased. The first series of bars represent the measurement results obtained in a soft car-to-car test whereas the tests at 40, 48 and 56km/h were all FFRB tests conducted with the dummy seated in the rear seat. The RibEye detected greater peak deflections than the potentiometer in all tests that were conducted at 56km/h. This confirms the greater out-of-plane motion that was observed in

the videos of the higher test speed tests. Figure 4 illustrates the effect of combined belt/ airbag loading in the two tests that were conducted with the dummy seated in the driver seat.

Crash videos were reviewed to determine the belt drape. Tests were classified, as having belt routing that was close to the neck, at the mid-shoulder and distal to the shoulder. RibEye measurements were normalized as a function of potentiometer measurement and plotted for both sides of the ribcage.

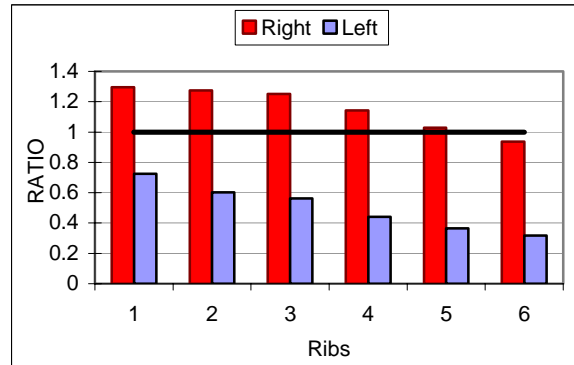


Figure 5: Potentiometer measure normalized to the individual RibEye deflection values for a belt that passes close to the neck. Left rear passenger.

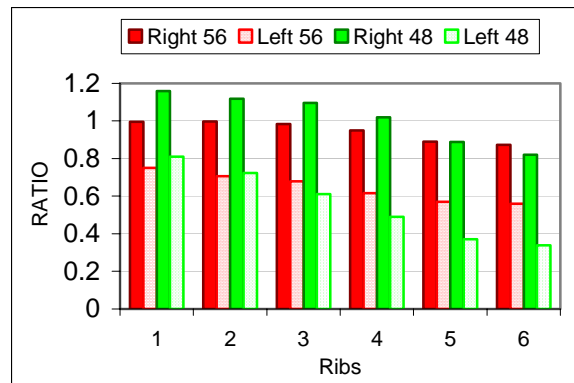


Figure 6: Potentiometer measure normalized to the individual RibEye deflection values for drivers with belt and airbag loading at 48 & 56 km/h.

Figure 5 is an example of the type of deflection pattern that is observed when the belt lies close to the neck. In this example the rear passenger dummy was seated behind the driver in a 40km/h FFRB test. The greatest rib deflection is observed on the right side of the rib cage. Figure 6 displays the deflection pattern observed when the belt and the airbag load the chest. In the 56km/h test the chest was evenly loaded however, in the vehicle that underwent the 48km/h test the videos confirmed that the shoulder belt was

very close to the neck resulting in higher peak upper rib deflections relative to the central potentiometer.

The RibEye system was able to consistently characterize the asymmetrical deformation of the chest for the belted loading conditions. An ATD seated behind the driver will have greater deflections on the right side of the chest as it rotates into the belt and outboard. Similarly for the passenger seated behind the front passenger, deflections will be greater on the left side of the thorax.

The system was found to track the belt position at peak load rather well. When the belt was close to the neck, the RibEye/ potentiometer ratio was greater than unity and progressively dropped in magnitude from the upper ribs down to the lower ribs. However, as the belt moved away from the neck and towards the middle of the shoulder, the normalized ratio for the lower ribs approached unity and was more evenly distributed from top to bottom. The sample contained only one vehicle model where the belt was clearly draped at the extremity of the shoulder. It was not possible therefore to draw any conclusion from this test since the lap belt penetrated the dummy abdomen.

Interference with the potentiometer resulted in data loss during the initial trials of the system. However the problem was rectified with a slight adjustment of the sensors. Data loss was also observed to occur occasionally in more severe test conditions with the lower rib channels. The data loss was likely related to the upward displacement of the abdominal insert.

Kinematic Analysis & Chest Deflection

Removal of the rear doors made it possible to obtain a full lateral view of the dummies as they engaged the seat cushion and restraint system in the rear seats. Generally the motion of the ATD's can be described as:

- a) Translation of the upper body and pelvis with minimal vertical motion; or
- b) Rotation of the upper body about the lap belt with large vertical displacement into the seat cushion.

The initial loading phase of the lumbar spine force appears to be a good indicator of these motions as each of these kinematic behaviors is associated with a distinctive time history trace. Figure 7 displays sample time history traces of the lumbar spine force in the vertical axis for three different vehicle seats associated with this motion. In the case of translation the vertical lumbar spine is in compression, early in the event as the pelvis and thighs of the dummy rapidly engage the seat cushion and belt. Extension of

the spine follows during rebound resulting in a clean sinusoidal trace. Figure 8 displays samples of time history traces for lumbar spine forces for four different vehicle seats wherein rotation was the principal motion. In these examples the lumbar spine is in extension at the onset of the loading phase. Observation of the videos suggests that this initial extension is characterized by a forward ramping of the pelvis; the dummy has less contact with the seat cushion and almost appears to become airborne in some cases. This motion early in the event contributes to spring-like oscillations of the dummy. The seatbelt and seat are discordant and there is substantially more out of plane motion than in the cases where translation is the predominant motion. Consequently, there is a greater tendency of lap belt migration into the abdominal cavity and greater opportunity for the head to strike the surrounding structure. The lumbar spine force response is dependant on seat and restraint system but does not appear to be affected by test severity.

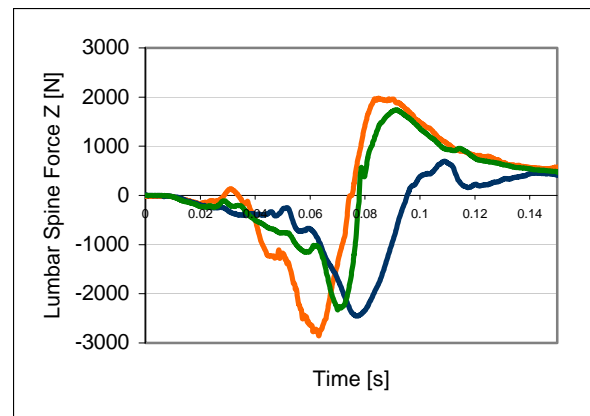


Figure 7: Time history traces of lumbar forces in dummies characterized by a translational motion in rear seats.

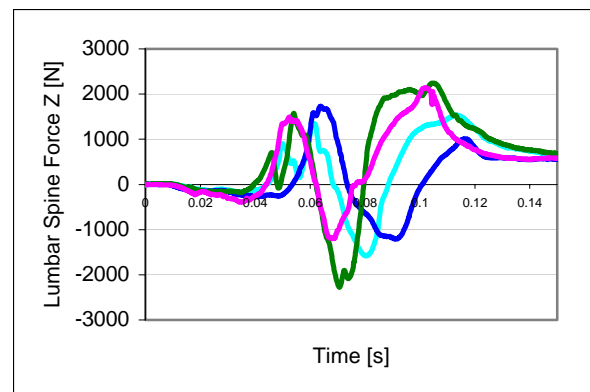


Figure 8: Time history traces of lumbar forces in dummies characterized by a rotational motion in rear seats.

The lumbar force time history may also be used to qualify, or explain the chest deflection measured at the potentiometer. The example shown in Figure 9 illustrates the interaction that occurs between chest deflection and the dummy kinematics. The time history traces presented are from a 56km/h test where the ATD was in the right front passenger seat. The chest deflection stops and remains constant at the moment that tension in the lumbar spine is released. There is no further deflection because the dummy is sliding downward into the seat. While this kinematic timing may be effective in reducing chest deflection, the risk of lap belt intrusion into the abdominal cavity may be increased.

Figure 10 illustrates the relationship between the lumbar spine forces and chest deflections at 48km/h and 56 km/h in the same vehicle model. As speed is increased the character of the traces remains unchanged but the magnitude is amplified. In this case the vertical force does not explain the observed difference in deflection.

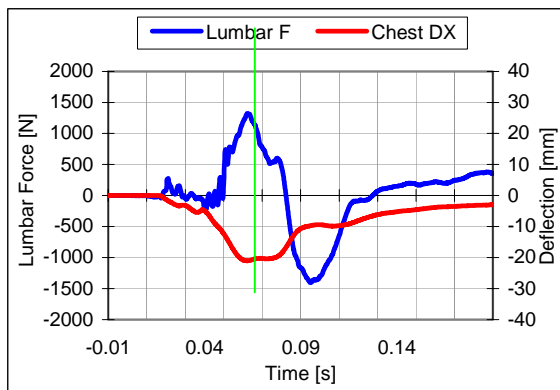


Figure 9: Time history trace of lumbar force and chest deflection for the front right passenger with seatbelt and airbag in a 56km/h FFRB test.

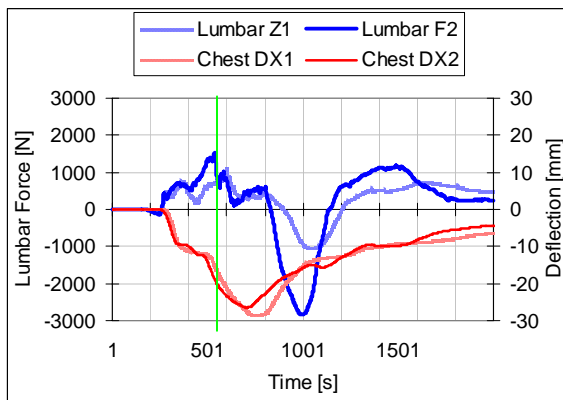


Figure 10: Time history trace of lumbar vertical force and chest deflection for the driver with belt/airbag in a 48 & 56km/h FFRB test.

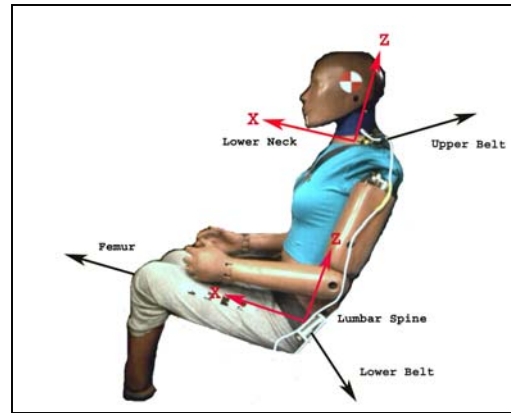


Figure 11: Free body diagram of forces included in the calculations.

Load Management

Comparison of dummy responses can be quite complex to carry out particularly when the dummies are in different vehicles, seat positions and exposed to different test speeds. Ideally, a comparison of the load distribution between the dummy and the restraint system could help quantify the energy management capabilities of a particular restraint system. Furthermore, qualification of load paths could help explain why deflection does not necessarily increase with increasing test speeds.

The individual force channels for the neck, pelvis, femurs, and lap and shoulder belt were integrated in time and summed as a function of time to provide an estimate of the total impulse in time. Figure 11 shows a free body diagram of the forces. Since this was a preliminary investigation calculations were restricted to two dimensions F_x and F_z . Comparisons were conducted with two FTSS 5th percentile Hybrid III dummies. The equations used for the calculations are presented in the Appendix.

Four separate comparisons will be presented as follows:

1. 2 drivers, 2 vehicle models;
2. Driver & passenger same vehicle crash;
3. Right front & right rear passengers same vehicle crash.
4. 2 drivers, same vehicle model two test speeds

The first sample includes a comparison of two dummies seated in the driver seat of two vehicles undergoing a FFRB test at 48 km/h. The dummies were each restrained by a seatbelt and an airbag. Figure 12 displays the loads on the belt in the solid color and the loads on the dummy in the shaded color. The test labeled as A and colored blue, indicates that more force was exerted on the dummy

than on the belt. In fact, the shoulder belt force, which was 3.5 kN for the driver was relatively low given that the chest was compressed to 38 mm. The driver clearly had femur contact with the knee bolsters since the femur loads were of the order of 4 kN in this test. In contrast, the belt forces for test B shown in red were significantly greater than the sum of the forces on the dummy. The dummy experienced very little load application. The seatbelt in this vehicle seems to have provided better energy management.

In the next plot, Figure 13 shows that the difference in chest deflections was 11 mm and that the chest in test A in blue was loaded more rapidly, more abruptly than in test B. In Figure 14, the third and final plot of the comparison, the two chest acceleration traces are overlaid, the blue trace or test A displays a more rapid drop and is noisier than the red trace of test B but the chest clips are equal. Overall the plots suggest that the restraint system in test B offered better chest protection.

The second sample is a comparison of a dummy in the driver seat and a dummy in the right front passenger seat of the same vehicle in a 56km/h FFRB test. Both dummies were restrained with the seatbelt and the airbag.

In Figure 15 the loads on the driver shown in shaded red are greater than the loads on the belt (solid red). The loads on the driver rose much more rapidly and were greater than the sum of the loads on the passenger shown in the shaded blue. The loads on the passenger belt shown by the solid blue trace were much greater than the loads on the passenger. The passenger therefore, appears to have exerted more force on the belt than the driver. The driver left femur load was above 8kN, the lumbar spine force was 3kN while the axial tension in the neck for the driver was above 2kN (N_{te} of 0.98) in this test, hence with such large loads transmitted above and below the chest it is not surprising to see that the chest was by-passed altogether.

Deflection for the driver, shown in red in Figure 16 was only 19 mm while for the passenger the chest deflection, shown in blue was 26 mm. Figure 17 displays the time history trace for the chest acceleration in red for the driver and in blue for the passenger. The onset of chest acceleration for both dummies were equal, however, beyond the initial peak the responses were quite different. The chest clip did not reflect the differences observed in the acceleration responses between the driver and passenger nor did they provide any indication that the load paths were away from the chest for driver and involved the chest for the passenger.

The third sample is a comparison of a dummy seated in the right front passenger seat with a dummy seated in the rear right passenger seat of a vehicle that underwent a FFRB test at 40 km/h. The front seat passenger is restrained with a seatbelt and airbag and the rear dummy is belted only.

Figure 18 illustrates the loads transmitted to the front passenger dummy in blue and the rear passenger dummy in red. Both belt load curves were well above the two dummy load curves. The sum of the dummy forces was slightly greater for the rear passenger but both dummy traces displayed a similar trend. This particular vehicle has firm seats and good belt geometry. The lumbar spine vertical forces for both the front and rear dummy are in compression early in the loading phase and there is good engagement between the pelvis and the seat cushion. The video analysis suggests a controlled deceleration of the dummies.

The deflections are shown in Figure 19. With the exception of the pretensioner response observed in the blue trace for the front passenger the shape of the traces were very similar. Deflection for the rear seat passenger shown in red was greater than for the front seat passenger seat by approximately 7 mm.

Figure 20 displays the chest acceleration traces, the pretensioner and load limiting effects of the front seatbelt shown in blue, cause a more gradual deceleration of the chest. Though the difference in chest clip is only 5g, the rear occupant is decelerated more rapidly and without interruption.

The final sample is a comparison of two dummies seated in the driver seats of two identical vehicle models tested in a 48 km/h and 56km/h FFRB crash. The blue traces represent the 48km/h test while the red trace represents the 56km/h test in all three graphs. Figure 21 indicates that the belt loads in both tests were comparable during the first 100 ms.. The sum of forces for the dummy was greater in the 56km/h test.

In Figure 22 the peak deflection measured at 56km/h, shown in red, was 26mm compared to 29mm for the 48km/h test. The chest acceleration traces in Figure 23 indicate a more rapid and slightly longer deceleration at 56km/h, yet there is only a 3g difference in chest clip.

While deflections were lower at 56km/h, the sum of impulses on the driver suggest that load paths were redirected to regions other than the chest in the higher severity crash test.

Sample 1

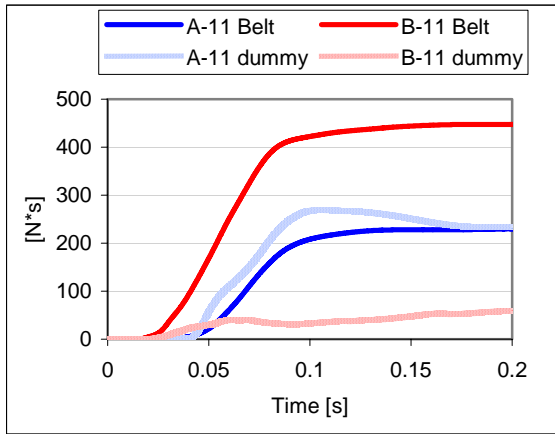


Figure 12: Comparison of load distribution for the dummy and the seatbelt for drivers in two 48km/h FFRB tests.

Sample 2

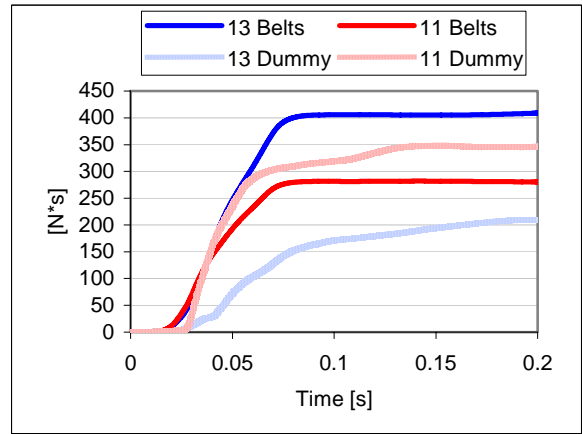


Figure 15: Comparison of load distribution for the dummy and the seatbelt for the driver and front passenger into a 56km/h FFRB test.

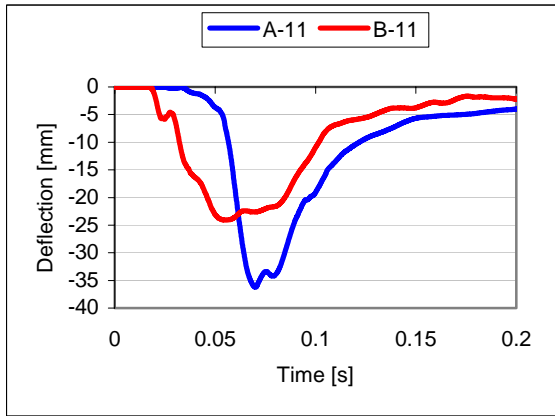


Figure 13: Corresponding chest deflections recorded in the two 48km/h FFRB tests.

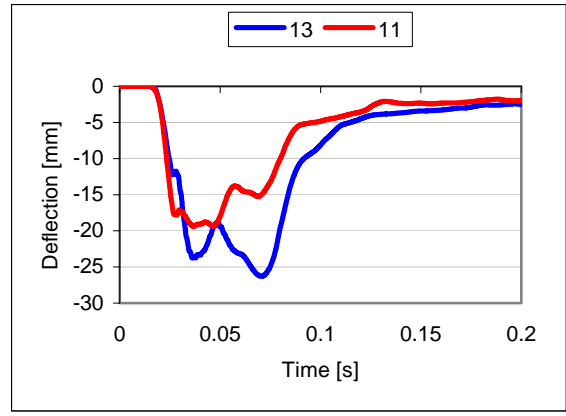


Figure 16: Corresponding chest deflection recorded in the 56km/h FFRB test.

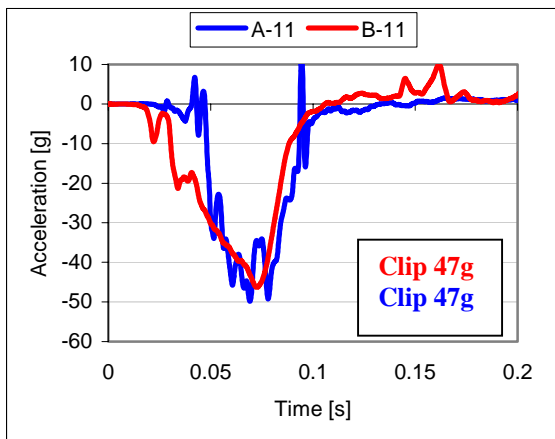


Figure 14: Corresponding chest accelerations recorded in the two 48km/h FFRB tests.

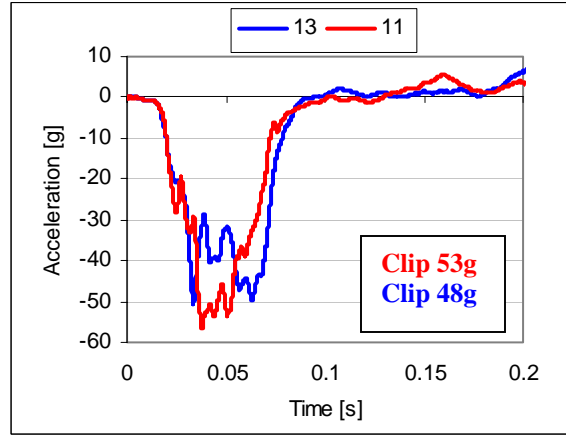


Figure 17: Corresponding chest accelerations recorded in the 56km/h FFRB test.

Sample 3

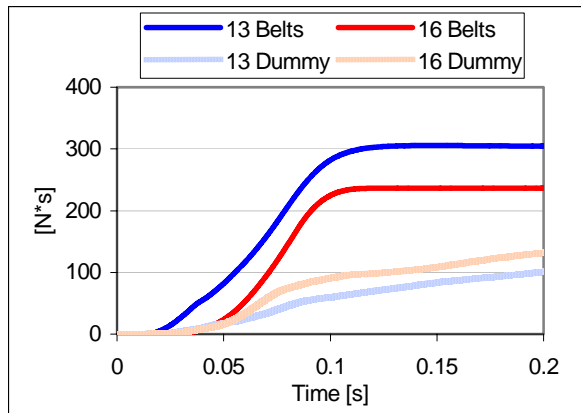


Figure 18: Comparison of load distribution for the dummy and the seatbelt for the right front and rear passenger in a 40km/h FFRB test.

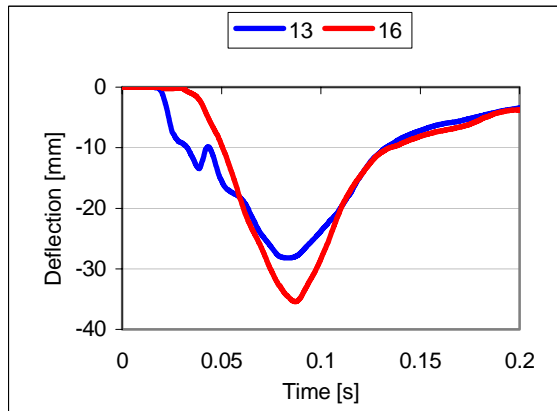


Figure 19: Corresponding chest deflections recorded in the 40km/h FFRB test.

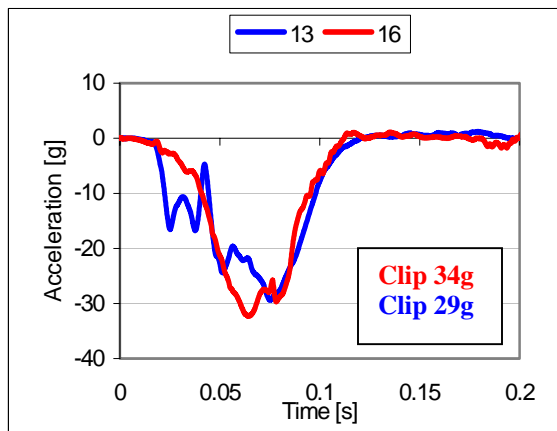


Figure 20: Corresponding chest accelerations recorded in the 40km/h FFRB test.

Sample 4

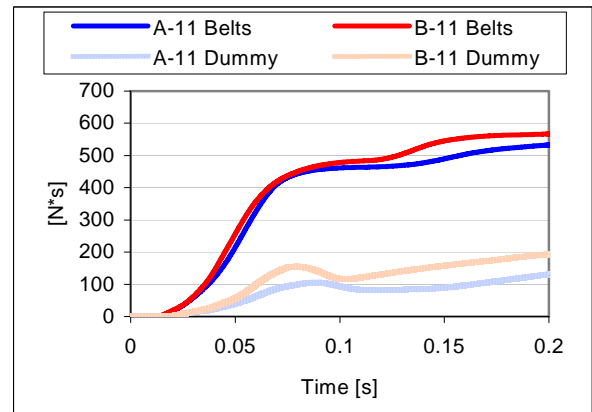


Figure 21: Comparison of load distribution for the dummy and the seatbelt for the drivers in 48km/h and 56km/h FFRB tests.

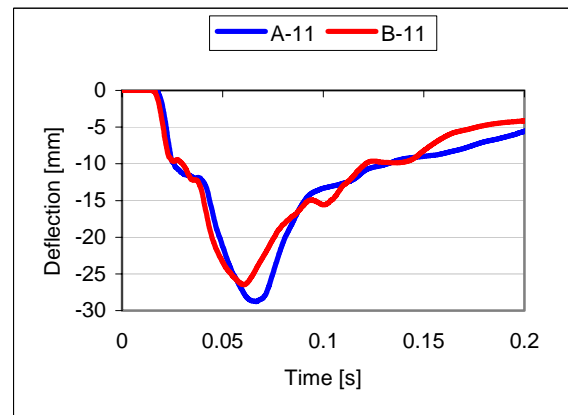
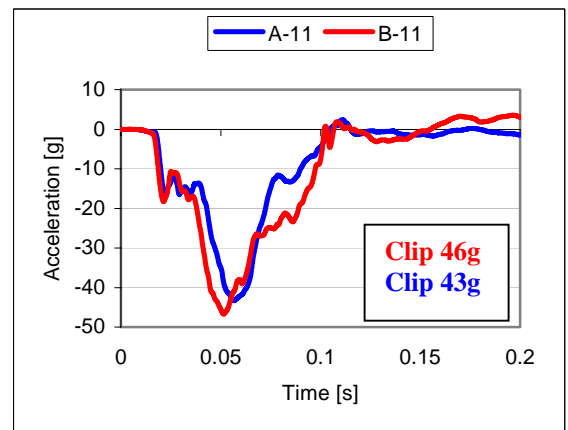


Figure 22: Corresponding chest deflections recorded in the 48km/h and 56km/h FFRB tests.



Corresponding chest accelerations recorded in the 48km/h and 56km/h FFRB tests.

DISCUSSION & CONCLUSION

Comparative testing with the Hybrid III 5th female dummy was conducted at 40, 48 and 56km/h to gain a better understanding of the effects of dummy kinematics and load distribution paths. New instrumentation capable of measuring deflection in two dimensions at 12 locations along the ribs of the dummy thorax will greatly facilitate the characterization of the chest response. The preliminary trials carried out in this test series suggest that this system could prove useful in delimiting belt routing on the chest. Asymmetrical loading particularly in more severe test conditions appears to be quantifiable with this system. Further testing under controlled conditions, should be conducted in order to determine where the sensors are best positioned to achieve optimal measurements. While the optical sensors require a clear line of sight, interference due to obstruction does not appear to be a problem unless belt intrusion and abdominal insert displacement occurs.

The lumbar spine force time history trace is a good indicator of seat and restraint performance. Video images confirm that lumbar force compression early in the event is associated with better seat cushion and seatbelt engagement and results in a more controlled deceleration. This signature trace is independent of test speed. Examination of the relationship between lumbar force and chest deflection time history traces can also, in certain vehicle models, help explain an unexpected reduction or increase in chest deflection since it reflects the vertical displacement of the dummy. Though not included in this study, the addition of anterior superior iliac spine load cells could provide a better definition of lap belt interaction with the pelvis and abdomen of the dummy.

The forces at the neck, lumbar spine and femurs were used to estimate the total impulse in time detected by the dummy and the total impulse in time measured in the seatbelt. Based on this exploratory exercise the method appears to offer the possibility of estimating the proportion of impulse from the crash that is directed to the dummy and the proportion transmitted to the belt. Measurements of direct load applications such as force and chest deflection are authoritative indicators of dummy load paths. Global measures such as acceleration clips provide only a snapshot in time and do not adequately describe the severity or duration of the loading event. The identification of load restrictions to key body regions could eventually provide a more comprehensive systems approach to the evaluation of occupant protection systems. Further applications of this method to a larger sample

of crashes will be completed to validate the process and establish correlation with existing injury criteria.

ACKNOWLEDGMENT

The authors would like to acknowledge Renault, Denton ATD and the staff of PMG Technologies for their assistance in the conduct of this study.

The opinions expressed and conclusions reached are solely the responsibility of the authors and do not necessarily represent the official policy of Transport Canada.

REFERENCES

- Canada Gazette Part I Department of Transport, Motor Vehicle Safety Act, Notice of Intent to Amend Section 208, 'Occupant Restraint Systems in Frontal Impact,' of the *Motor Vehicle Safety Regulations*" June 30, 2001, page 2359.
- Tylko S., Charlebois, D., Bussières, A., Dalmotas, D., The Effect Of Breast Anthropometry On The Hybrid III 5th Female Chest Response, Stapp Car Crash Journal, Vol. 50 (November 2006)

APPENDIX

Impulse calculation equations:

$$pulseZ(t_i) = \sum_{t=0}^{t=0.2} \left[\int_t^{t+i} F_{z,neck} + \int_t^{t+i} F_{z,lumbar} \right]$$

$$pulseX(t_i) = \sum_{t=0}^{t=0.2} \left[\int_t^{t+i} F_{x,neck} + \int_t^{t+i} F_{x,lumbar} + \int_t^{t+i} F_{femur} \right]$$

$$pulseDummy(t_i) = \sqrt{pulseX^2 + pulseZ^2}$$

$$pulseBelt(t_i) = \sum_{t=0}^{t=0.2} \left[\int_t^{t+i} F_{LAP} + \int_t^{t+i} F_{UPPER} \right]$$